



Calorimetric determination of the upper critical fields and anisotropy of NdFeAsO_{1-x}F_x single crystals

U. Welp,¹ R. Xie,^{1,2} A. E. Koshelev,¹ W. K. Kwok,¹ P. Cheng,³ L. Fang,³ and H.-H. Wen³

¹Materials Science Division, Argonne National Laboratory, Argonne, Illinois 60439, USA

²Department of Physics, University of Notre Dame, Notre Dame, Indiana 46556, USA

³Institute of Physics, Chinese Academy of Sciences, Beijing 100190, People's Republic of China

(Received 26 July 2008; revised manuscript received 25 August 2008; published 30 October 2008)

We present heat-capacity measurements of the upper critical fields of single-crystal NdFeAsO_{1-x}F_x. In zero-magnetic field a clear step in the heat capacity is observed at $T_c \approx 47$ K. In fields applied perpendicular to the FeAs layers the step broadens significantly whereas for the in-plane orientation the field effects are small. This behavior is reminiscent of the CuO₂-high- T_c superconductors and is a manifestation of pronounced fluctuation effects. Using an entropy conserving construction we determine the transition temperatures in applied fields and the upper critical-field slopes of $\partial H_{c2}^c / \partial T = -0.72$ T/K and $\partial H_{c2}^{ab} / \partial T = -3.1$ T/K. Zero-temperature coherence lengths of $\xi_{ab} \approx 3.7$ nm and $\xi_c \approx 0.9$ nm and a modest superconducting anisotropy of $\lambda \sim 4$ can be deduced in a single-band model.

DOI: [10.1103/PhysRevB.78.140510](https://doi.org/10.1103/PhysRevB.78.140510)

PACS number(s): 74.25.Dw, 74.70.-b

The recent discovery of superconductivity in LaFeAsO_{1-x}F_x (Ref. 1) has led to the emergence of a family of layered high-temperature superconductors with compositions RFeAsO_{1-x}F_x with rare earths R=Sm, Ce, Nd, Pr, Gd, Tb, and Dy. Currently, the highest value of T_c is 55 K.² These materials have a layered tetragonal crystal structure¹ in which the FeAs layers are believed to carry superconductivity, whereas the RO_{1-x}F_x layers serve as charge reservoirs. The undoped parent compounds [LaFeAsO,³ NdFeAsO,⁴ and CeFeAsO (Ref. 5)] are semimetals that undergo a tetragonal-to-orthorhombic transition near 150 K and enter an antiferromagnetically ordered state at lower temperature. Upon electron doping through substitution of O with F or hole doping through substitution of R with Sr (Ref. 6), the structural and the antiferromagnetic transitions are suppressed and a superconducting state emerges resulting in an intriguing interplay of magnetism and superconductivity reminiscent of the behavior of the cuprate high- T_c superconductors. Furthermore, electronic band-structure calculations^{7,8} indicate that the Fermi surface contains multiple sheets derived from the Fe d orbitals, which could give rise to multiband superconductivity.⁹⁻¹¹

The upper critical field H_{c2} and its anisotropy are fundamental characteristics that shed light on these microscopic properties of the FeAs superconductors. To date, H_{c2} has been inferred mostly from transport measurements on polycrystalline samples. Here we present a thermodynamic determination of the upper critical fields of single-crystal NdFeAsO_{1-x}F_x using heat-capacity measurements. In zero-magnetic field a clear step in the heat capacity is observed at $T_c \approx 47$ K. In fields applied perpendicular to the FeAs layers the step broadens significantly, whereas for the in-plane orientation the field effects are small. This behavior is reminiscent of the CuO₂-high- T_c superconductors and is a manifestation of pronounced fluctuation effects. Using an entropy conserving construction we determine the transition temperatures in applied fields and the upper critical-field slopes of $\partial H_{c2}^c / \partial T = -0.72$ T/K and $\partial H_{c2}^{ab} / \partial T = -3.1$ T/K. These values are significantly lower than previous resistive

determinations.^{12,13} Zero-temperature coherence lengths of $\xi_{ab} \approx 3.7$ nm and $\xi_c \approx 0.9$ nm and a modest superconducting anisotropy of $\gamma \sim 4$ can be deduced in a single-band model.

The crystals used in this study have a nominal composition of $x=0.18$ and were grown from a NaCl flux as described in Ref. 12. We performed the caloric measurements using a membrane-based steady-state ac microcalorimeter.¹⁴ It utilizes a thermocouple composed of Au-1.7% Co and Cu films deposited onto a 150-nm-thick Si₂N₄ membrane as thermometer. Ten NdFeAsO_{1-x}F_x crystallites of various sizes were mounted onto the thermocouple using minute amounts of Apiezon N grease (see inset of Fig. 3). An ac-heater current at 47 Hz is adjusted such as to induce oscillations of the sample temperature of 50–200 mK. The ac technique is very sensitive for detecting changes in the specific heat, but less so for the determination of absolute values. This is particularly true in the present case where—because of the small sample size—the signal due to superconductivity amounts to only a fraction of 1×10^{-3} of the total signal. Therefore, we concentrate here on tracing the superconducting phase boundaries and the anisotropy.

Figure 1 shows the superconducting part of the heat-capacity signal for various fields applied along the c axis and the ab plane, respectively. These data are obtained by subtracting from each measurement the normal-state background c_n , which includes contributions from phonons, normal electrons, and possibly magnetism, and the addenda. We use the data in a magnetic field of 7.5 T applied along the c axis as background. These data follow a smooth curve which we fitted in the temperature range of 30–60 K with a fifth order polynomial resulting in uniformly distributed residuals. In order to minimize noise, we used this polynomial as a background signal for the $H \parallel c$ and the $H \parallel ab$ data. This choice of background is suitable for the high-temperature part of the phase diagram. In zero field a clear step with onset near 48 K and a peak near 46 K is observed. These temperature values are in reasonable agreement with the onset and zero-resistance temperatures seen in the resistive transitions of similar crystals.¹² The absence of any addi-

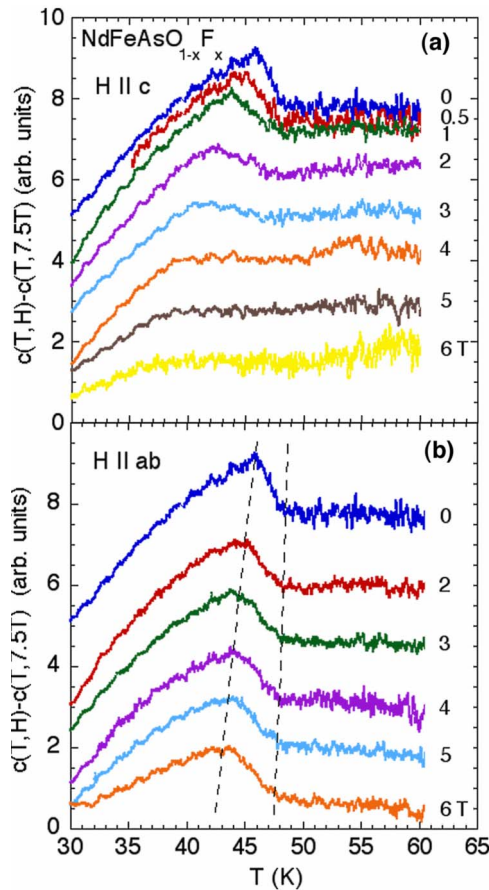


FIG. 1. (Color online) Temperature dependence of the heat capacity $c(T, H) - c(T, 7.5 \text{ T} \parallel c)$ in various fields applied perpendicular and parallel to the FeAs layers. The dashed lines indicate the shift of the peak and onset with increasing fields applied along the planes.

tional structure in the heat-capacity transition indicates that the transition width observed in our measurements is not caused by an average over several crystallites with individual sharp transitions but that it is an inherent property of the current material. With increasing field along the c axis the heat-capacity anomaly broadens significantly and its height decreases rapidly. In fields higher than $3 \text{ T} \parallel c$ the step has essentially disappeared and the peak has transformed into a kink that can be traced up to 6 T . In contrast, for fields applied along the ab directions the specific-heat step stays well defined and shifts slightly to lower temperatures as indicated by the dashed lines. This general behavior is similar to observations on CuO_2 high- T_c superconductors,¹⁵ but is markedly different from MgB_2 ,¹⁶ which has similar values of T_c and anisotropy as $\text{NdFeAsO}_{1-x}\text{F}_x$. The systematic vertical displacement of the curves in Fig. 1 is caused most likely by the field dependence of the large addendum contribution to the heat capacity.

The data in Fig. 1 allow the construction of the anisotropic superconducting phase diagram of $\text{NdFeAsO}_{1-x}\text{F}_x$ as shown in Fig. 2. We define the transition temperature $T_{c2}(H)$ through an entropy conserving construction¹⁷ as illustrated in Fig. 3. Figure 2 also shows the field dependence of the temperature T_p of the peak or kink in $c(T)$. The average slopes of

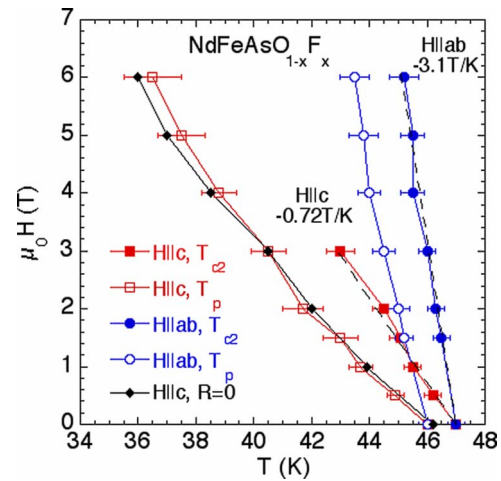


FIG. 2. (Color online) Phase diagram of $\text{NdFeAsO}_{1-x}\text{F}_x$ as determined from field dependence of the peak positions and of T_{c2} . The dashed lines are linear fits yielding the average upper critical-field slopes of -3.1 and -0.72 T/K for the ab plane and c axes, respectively. Also included are the zero-resistance points in fields along the c axis obtained on similar crystals (Ref. 12).

H_{c2} for the c and ab axes, respectively, are $\partial H_{c2}^c / \partial T = -0.72 \text{ T/K}$ and $\partial H_{c2}^{ab} / \partial T = -3.1 \text{ T/K}$ resulting in a modest superconducting anisotropy of $\gamma \sim 4.3$. Using the Ginzburg-Landau relations for the upper critical field, $H_{c2}^c = \phi_0 / 2\pi\xi_{ab}^2$

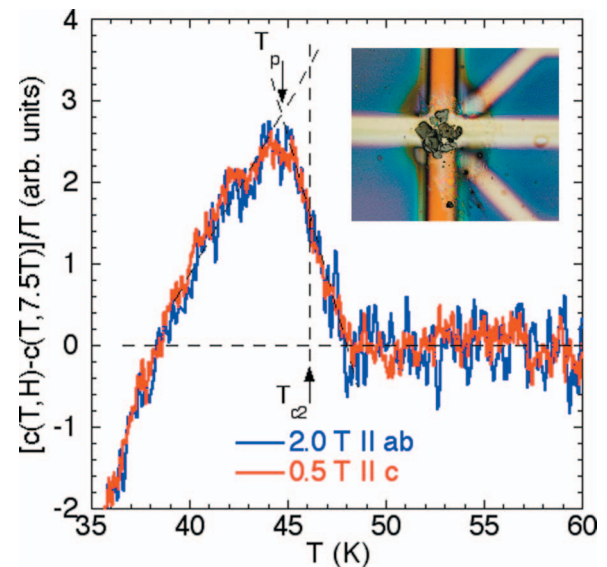


FIG. 3. (Color) Superconducting heat capacity divided by temperature in $2 \text{ T} \parallel ab$ and $0.5 \text{ T} \parallel c$. The dashed lines indicate the definitions of T_p and T_{c2} . T_{c2} is determined by approximating the measured broad transition with an ideal steplike transition (Refs. 15 and 17). Then, entropy conservation requires that the triangular areas above and below the measured traces are equal. The inset shows the $\text{NdFeAsO}_{1-x}\text{F}_x$ crystallites mounted on the calorimeter. The crystallites are thin plates with in-plane dimensions of up to $\sim 50 \mu\text{m}$ and thickness of about $2 \mu\text{m}$. The Si_3N_4 membrane appears in blue, the Cu and Au/Co legs of the thermocouple are the vertical and horizontal metal films, and the diagonal lines are contacts to the meander heater located underneath the junction. The width of the thermocouple legs is about $100 \mu\text{m}$.

and $H_{c2}^{ab} = \phi_0 / 2\pi \xi_{ab} \xi_c$, and the single-band Werthamer-Helfand-Hohenberg (WHH) expression relating the zero-temperature upper critical field to the slope at T_c , $H_{c2}(0) = -0.69 T_c (\partial H_{c2} / \partial T)_{T_c}$; we obtain the following parameters for our NdFeAsO_{1-x}F_x samples: $H_{c2}^c(0) \approx 23$ T, $H_{c2}^{ab}(0) \approx 100$ T, $\xi_c(0) \approx 0.9$ nm, and $\xi_{ab} \approx 3.7$ nm. As a reference point, the paramagnetic limiting field H_p has a value of $H_p[T] = 1.84 \cdot T_c[K] = 86.5$ T which is slightly below our estimate of H_{c2}^{ab} . Previous determinations of the upper critical field of NdFeAsO_{1-x}F_x using magnetotransport measurements on polycrystalline¹³ and single-crystal¹² samples have yielded significantly larger H_{c2} values. From transport measurements on crystals upper critical-field slopes of -1.85 and -9 T/K were observed for the c axis and ab plane, respectively. We attribute this difference to the uncertainty in assigning a resistivity criterion for the determination of H_{c2} (Ref. 18) when the transitions broaden strongly in a magnetic field. We note though that the zero-resistance points for $H \parallel c$ obtained on similar crystals¹² coincide well with T_p , that is, the completion of the transition. Furthermore, the anisotropy parameter deduced from the single-crystal transport measurements¹² is close to the value obtained here. This is consistent with the observation that the anisotropy factor deduced from our caloric measurements does not depend on the definition of the superconducting transition, i.e., T_p or T_{c2} , as demonstrated directly in Fig. 3. The data for the entire transition taken in 0.5 T $\parallel c$ superimpose very well onto those taken in 2 T $\parallel ab$, indicating that the anisotropy is close to $\gamma \sim 4$. Our data do not reveal—at least in the temperature range close to T_c presented here—a temperature dependence of γ as has been recently observed in torque measurements on SmFeAsO_{1-x}F_x (Ref. 11) and in the flux flow resistance of NdFeAsO_{1-x}F_x.¹⁹ Our findings of a temperature-independent anisotropy of $\gamma \sim 4$ are in good agreement with results of recent rf screening experiments.²⁰

The angular-dependent transition temperature $T_{c2}(\theta)$ is given by $T_{c2}(\theta) = T_{c0} + H \sqrt{\cos^2(\theta) + \gamma^2 \sin^2(\theta)} / (\partial H_{c2}^{ab} / \partial T)$ within the effective-mass model of the Ginzburg-Landau theory of anisotropic superconductors, assuming linear phase boundaries. Here, θ is the angle of the magnetic field with respect to the FeAs planes and T_{c0} is the zero-field transition temperature. Figure 4 shows the angular dependence of the transition temperature in 1.5 T together with a fit according to the effective-mass model. Within the experimental uncertainties the data are well described by an anisotropy coefficient of $\gamma \sim 4$ consistent with the discussion above. A mosaic spread due to the mounting of the crystallites could cause a reduced measured anisotropy. However, we estimate the possible misalignment to be less than 5° , which would not affect the determination of γ in a significant way.

Electronic band-structure calculations⁷ have revealed five Fermi-surface sheets, two high-velocity cylindrical electron sheets centered on the line between the high-symmetry points M and A of the tetragonal Brillouin zone, two low-velocity cylindrical hole sheets centered on the ΓZ line, and a three-dimensional heavy-hole pocket centered on the Z point. An over-all effective-mass anisotropy $m_c/m_{ab} = (\xi_{ab}/\xi_c)^2 = \gamma^2$ of ~ 15 is found, which depends on the electron-doping level. The good agreement with our experimental value for the superconducting anisotropy might be

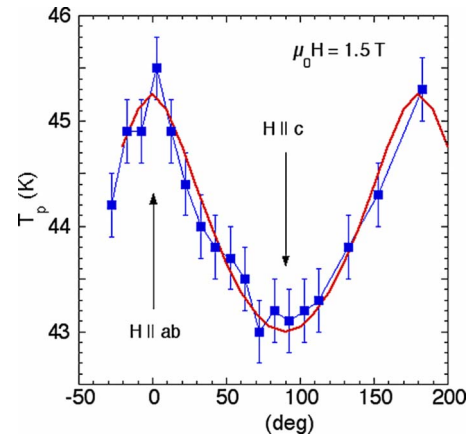


FIG. 4. (Color online) Angular dependence of the peak temperature in a field of 1.5 T. The solid line is a fit with an anisotropy of $\gamma = 4$.

somewhat fortuitous; however, the results obtained here may serve as reference point for future refinements of the calculations.

The evolution of the heat capacity in applied fields shown in Fig. 1 can be attributed to the effects of superconducting fluctuations. The importance of fluctuations in zero-magnetic field is quantified by the Ginzburg number $G_i = (k_B T_{c0} / H_c^2 \xi_{ab}^2 \xi_c^2) / 2 = (8 \pi^2 k_B T_{c0} \lambda_{ab}^2 / \phi_0^2 \xi_c^2) / 2$. k_B , ϕ_0 , H_c , and λ_{ab} are the Boltzmann constant, flux quantum, thermodynamic critical field, and in-plane magnetic penetration depth, respectively. Using the above estimate for ξ_c and a typical value of $\lambda_{ab} \sim 200$ nm (Refs. 20 and 21) we obtain $G_i \sim 2 \cdot 10^{-3}$. This value is lower than that for CuO₂-high- T_c superconductors ($G_i \sim 10^{-2} - 1$) but is about ten times larger than the value for single-crystal MgB₂. In high-applied fields the transition progressively broadens due to enhanced fluctuations as expressed by a field-dependent Ginzburg number $G_i(H) = (4 \pi k_B T_{c0} H / \phi_0 \xi_c H_c^2)^{2/3}$ (Ref. 22) which would yield a temperature range of ~ 2 K of strong fluctuations in a field of 5 T.

The analysis presented above, in particular the extrapolation of the zero-temperature values, is valid for a single-band BCS superconductor. The deviations of the resistively determined upper critical field of polycrystalline LaFeAsO_{1-x}F_x (Ref. 9) at high fields from the expected single-band WHH variation, the temperature-dependent superconducting anisotropy of SmFeAsO_{1-x}F_x crystals¹¹ from magnetic torque and from flux flow in NdFeAsO_{1-x}F_x crystals,¹⁹ as well as the presence of multiple iron d bands at the Fermi energy^{7,8} have led to the suggestion that the FeAs superconductors could be two (multiple) band superconductors. Even though the temperature dependence of T_p for $H \parallel c$ gives some indication for upward curvature, the limited temperature range and the experimental uncertainties of the present data preclude a definite conclusion.

In summary, we have determined the upper critical field of single-crystal NdFeAsO_{1-x}F_x using heat-capacity measurements. The upper critical-field slopes are $\partial H_{c2}^c / \partial T = -0.72$ T/K and $\partial H_{c2}^{ab} / \partial T = -3.1$ T/K, which correspond—in

a single-band model—to zero-temperature coherence lengths of $\xi_{ab} \approx 3.7$ nm and $\xi_c \approx 0.9$ nm and a modest superconducting anisotropy of $\gamma \sim 4$. This anisotropy parameter is in good agreement with recent band-structure calculations. In fields applied parallel to the c axis the superconducting transition broadens significantly indicative of pronounced fluctuation effects. Therefore, we expect the appearance of an extended vortex liquid state and—in sufficiently clean samples—a vortex lattice melting transition, which are hall

marks of the phase diagram of the CuO_2 -high- T_c superconductors.²³

This work was supported by the U.S. Department of Energy–Basic Energy Science—under Contract No. DE-AC02-06CH11357, by the Natural Science Foundation of China, by the Ministry of Science and Technology of China (973 under Projects No. 2006CB60100, No. 2006CB921802 and No. 2006CB921107), and by the Chinese Academy of Sciences (Project ITSNEM).

- ¹Y. Kamihara, T. Watanabe, M. Hirano, and H. Hosono, *J. Am. Chem. Soc.* **130**, 3296 (2008); H. Takahashi, K. Igawa, K. Arii, Y. Kamihara, M. Hirano, and H. Hosono, *Nature (London)* **453**, 376 (2008).
- ²Z.-A. Ren *et al.*, *Chin. Phys. Lett.* **25**, 2385 (2008).
- ³C. de la Cruz *et al.*, *Nature (London)* **453**, 899 (2008); M. McGuire, A. Christianson, A. Sefat, B. Sales, M. Lumsden, R. Jin, E. Andrewpayzant, D. Mandrus, Y. Luan, V. Keppens, V. Varadarajan, J. Brill, R. Hermann, M. Sougrati, F. Grandjean, and G. Long, *Phys. Rev. B* **78**, 094517 (2008).
- ⁴Y. Qiu, W. Bao, Q. Huang, T. Yildirim, J. Simmons, J. Lynn, Y. Gasparovic, J. Li, M. Green, T. Wu, G. Wu, and X. Chen, arXiv:0806.2195 (unpublished).
- ⁵J. Zhao, Q. Huang, C. de la Cruz, S. Li, J. Lynn, Y. Chen, M. Green, G. Chen, G. Li, Z. Li, J. Luo, N. Wang, and P. Dai, arXiv:0806.2528 (unpublished); G. F. Chen, Z. Li, D. Wu, G. Li, W. Z. Hu, J. Dong, P. Zheng, J. L. Luo, and N. L. Wang, *Phys. Rev. Lett.* **100**, 247002 (2008).
- ⁶H. H. Wen *et al.*, *Europhys. Lett.* **82**, 17009 (2008).
- ⁷D. J. Singh and M. H. Du, *Phys. Rev. Lett.* **100**, 237003 (2008).
- ⁸S. Lebegue, *Phys. Rev. B* **75**, 035110 (2007).
- ⁹V. Cvetkovic and Z. Tesanovic, arXiv:0804.4678 (unpublished).
- ¹⁰F. Hunte *et al.*, *Nature (London)* **453**, 903 (2008).
- ¹¹S. Weyeneth, U. Mosele, N. Zhigadlo, S. Katrych, Z. Bukowski, J. Karpinski, S. Kohout, J. Roos, and H. Keller, arXiv:0806.1024 (unpublished).
- ¹²Y. Jia *et al.*, *Appl. Phys. Lett.* **93**, 032503 (2008).
- ¹³X. L. Wang, R. Ghorbani, G. Peleckis, and S. X. Dou, arXiv:0806.0063 (unpublished); D. Wu *et al.*, *Sci. China, Ser. G* **51**, 715 (2008).
- ¹⁴A. Rydh, in *Encyclopedia of Materials: Science and Technology*, edited by K. H. J. Buschow, M. C. Flemings, R. W. Cahn, P. Veysière, E. J. Kramer, and S. Mahajan (Elsevier, Oxford, 2006); Available online at <http://www.sciencedirect.com/science/referenceworks/0080431526>
- ¹⁵E. Bonjour, R. Calemczuk, J. Y. Henry, and A. F. Khoder, *Phys. Rev. B* **43**, 106 (1991); A. Junod *et al.*, *Physica C* **211**, 304 (1993); A. Schilling, R. A. Fisher, N. E. Phillips, U. Welp, W.-K. Kwok, and G. W. Crabtree, *Phys. Rev. Lett.* **78**, 4833 (1997).
- ¹⁶L. Lyard, P. Samuely, P. Szabo, T. Klein, C. Marcenat, L. Paulius, K. H. P. Kim, C. U. Jung, H. S. Lee, B. Kang, S. Choi, S. I. Lee, J. Marcus, S. Blanchard, A. G. M. Jansen, U. Welp, G. Karapetrov, and W. K. Kwok, *Phys. Rev. B* **66**, 180502(R) (2002); A. Rydh *et al.*, *ibid.* **70**, 132503 (2004).
- ¹⁷N. E. Phillips and R. A. Fisher, *Chin. J. Phys. (Taipei)* **30**, 799 (1992); J. Kacmarcik *et al.*, *Acta Phys. Pol. A* **113**, 363 (2008); S. B. Ota, V. S. Sastry, E. Gmelin, P. Murugaraj, and J. Maier, *Phys. Rev. B* **43**, 6147 (1991).
- ¹⁸U. Welp, W.-K. Kwok, G. W. Crabtree, K. G. Vandervoort, and J. Z. Liu, *Phys. Rev. Lett.* **62**, 1908 (1989).
- ¹⁹Y. Jia *et al.*, *Supercond. Sci. Technol.* **21**, 105018 (2008).
- ²⁰C. Martin, R. Gordon, M. Tanatar, M. Vannette, M. Tillman, E. Mun, P. Canfield, V. Kogan, G. Samolyuk, J. Schmalian, and R. Prozorov, arXiv:0807.0876 (unpublished).
- ²¹H. Luetkens, H.-H. Klauss, R. Khasanov, A. Amato, R. Klingeler, I. Hellmann, N. Leps, A. Kondrat, C. Hess, A. Kohler, G. Behr, J. Werner, and B. Buchner, *Phys. Rev. Lett.* **101**, 097009 (2008); R. Khasanov, H. Luetkens, A. Amato, H. Klauss, Z. Ren, J. Yang, W. Lu, and Z. Zhao, *Phys. Rev. B* **78**, 092506 (2008); A. Narduzzo, M. Grbic, M. Pozek, A. Dulcic, D. Paar, A. Kondrat, C. Hess, I. Hellmann, R. Klingeler, J. Werner, A. Kohler, G. Behr, and B. Buchner, *Phys. Rev. B* **78**, 012507 (2008); A. J. Drew, F. L. Pratt, T. Lancaster, S. J. Blundell, P. J. Baker, R. H. Liu, G. Wu, X. H. Chen, I. Watanabe, V. K. Malik, A. Dubroka, K. W. Kim, M. Rössle, and C. Bernhard, *Phys. Rev. Lett.* **101**, 097010 (2008).
- ²²R. Ikeda, T. Ohmi, and T. Tsuneto, *J. Phys. Soc. Jpn.* **58**, 1377 (1989); U. Welp, S. Fleshler, W. K. Kwok, R. A. Klemm, V. M. Vinokur, J. Downey, B. Veal, and G. W. Crabtree, *Phys. Rev. Lett.* **67**, 3180 (1991).
- ²³W. K. Kwok, S. Fleshler, U. Welp, V. M. Vinokur, J. Downey, G. W. Crabtree, and M. M. Miller, *Phys. Rev. Lett.* **69**, 3370 (1992); E. Zeldov, D. Majer, M. Konczykowski, V. B. Geschkenbein, V. M. Vinokur, and H. Shtrikman, *Nature (London)* **375**, 373 (1995); A. Schilling *et al.*, *ibid.* **382**, 791 (1996).